ELSEVIER

Sedimentary Geology 137 (2000) 107–126

Sedimentary Geology

www.elsevier.nl/locate/sedgeo

Iron bacterial and fungal mats, Bajocian stratotype (Mid-Jurassic, northern Normandy, France)

A. Préat[a,*], B. Mamet[a], C. De Ridder[b], F. Boulvain[c], D. Gillan[b]

[a]*Département des Sciences de la Terre et de l'Environnement CP160/02, Université Libre de Bruxelles, 50 av. Roosevelt B-1050 Brussels, Belgium*
[b]*Laboratoire de Biologie Marine CP160/15, Université Libre de Bruxelles, 50 av. Roosevelt B-1050 Brussels, Belgium*
[c]*Géologie-Pétrologie-Géochimie, B20, Université de Liège, Sart Tilman B-4000 Liège, Belgium*

Received 23 September 1999; accepted 19 May 2000

Abstract

The Oolithe ferrugineuse de Bayeux Formation is located at the historical Bajocian stratotype of Sainte-Honorine-des-Pertes, north of Bayeux, Normandy. The condensed formation ranges from the base of the *Humphriesianum* Zone to the *Parkinsoni* Zone and is divided into four beds of decimetric scale.

Three main microfacies are present: (1) oncoid rudstones, (2) ooid bioclastic packstones and (3) silty burrowed wackestones/packstones. Sedimentation took place in a very quiet environment, below the photic zone and below or near the storm wave base. The general setting is a distal carbonate ramp, its lower part characterized by hemipelagic sedimentation indicated by the presence of planktonic foraminifers. The inferred depth is around 100 m. Free oxygen concentration was low. Dysaerobic conditions are indicated by a scarcity of benthic macrofauna.

Ferruginous structures are numerous in the first two microfacies, and absent in the last. Hematite staining is not uniform and follows many sedimentary patterns. Among the more widespread Fe structures are perforation infillings with endolithic microorganisms, microstromatolites, oncoids, ooids, blisters, coatings and hardgrounds. These structures can be associated and none are mutually exclusive. Hematite-coated filaments of different sizes and shapes are observed in the micrite matrix: the walls of various organisms; the calcite crystals associated with the Fe cortical laminations; the perforations and burrow; the hardgrounds; and microstromatolites. Petrographical and SEM examinations suggest that the laminated crusts (oncoids and hardgrounds) are formed by microbial iron mats dominated by filamentous bacteria and fungi. Seven types of microbes are recognized: filaments (five morphotypes), spheroidal bodies and stalked bodies. Filamentous microfossils of type 1 to 4 resemble the present-day filamentous bacteria (Beggiatoales and Cytophagaceae). Because of their large diameter and their branching nature, filaments of type 5 are possibly filamentous fungi. Another argument in favor of fungi is the presence of stalked and spheroidal bodies that resemble zoosporangia and oogonia of some Oomycota.

In deep, calm and dysaerobic waters, many interfaces (e.g. between aerobic and dysaerobic waters) are present in the sediments. The stability of the soluble reduced state of iron (Fe^{2+}) is higher at such interfaces, and many ferric iron-encrusted microbial fossils are observed. Iron could thus serve as an electron donor for microbial iron-oxidation processes. Other microbial iron deposition pathways are also possible.

* Corresponding author. Fax: +32-2-650-2226.
E-mail address: apreat@ulb.ac.be (A. Préat).

PII: S0037-0738(00)00101-9

It appears that, regardless of geological age (Paleozoic, Mesozoic) and geographical location, the same microbiological mechanisms are probably responsible for the red color in calcareous stratified or unstratified bodies. The presence of fossilized iron-encrusted bacteria and fungi at interfaces may therefore serve as an indicator of anoxic to dysaerobic conditions in various paleo(micro)environments.

Keywords: Biogeochemistry; Iron-microbes; Fe oncoids; Condensed series; Jurassic

1. Introduction

The Oolithe ferrugineuse de Bayeux is the historical Bajocian stratotype at Sainte-Honorine-des-Pertes, Bayeux, Normandy (d'Orbigny, 1849–1852; Rioult, 1964). The formation (0.05–0.5 m thick) is condensed and ranges from the base of the *Humphriesianum* to the *Parkinsoni* Zones (Rioult et al., 1991; Gauthier et al., 1995) (Fig. 1). Sedimentological analysis by Rioult et al. (1991) provides a general sequence stratigraphic interpretation on a regional scale. The formation is divided into four decimetric beds that contain centimetric rounded ferruginous oncoids, ferruginous stromatolite pavements and abundant well-sorted ferruginous ooids. Dangeard (1930) and Rioult (1964) describe 'algal filaments' from these Jurassic ferruginous nodules. Fürsich (1971) was the first to describe multiple hardgrounds in the formation and to highlight the role of condensation. Gatrall et al. (1972) studied ferruginous concretions in contemporary sections from southern England (Dorset and Somerset), and their findings support an abiotic as well as a biotic (algal) precipitation. However, Palmer and Wilson (1990) found that the ferruginous nodules of England formed under the influence of non-photosynthetic, iron-oxidizing bacteria. Despite these controversial studies, the origin of the localized iron concentration remains unclear (Nealson, 1983; Fortin et al., 1997; Chafetz et al., 1998; Konhauser, 1998).

We have recently described iron-encrusted microorganisms from several red European Paleozoic series (Mamet and Boulvain, 1988, 1991; Boulvain, 1989, 1993; Bourque and Boulvain, 1993; Mamet and Perret, 1995; Mamet et al., 1997; Préat et al., 1998; Préat et al., 1999a,b). Bacteria are also present in a ferric biofilm on the shell of a burrowing bivalve (*Montacuta ferruginosa*) that lives in the Recent intertidal sediments of northern France (Gillan and De Ridder, 1995, 1997; Gillan et al., 2000). In these studies, most of the iron is believed to be the result of a microbially induced precipitation. It is therefore significant to determine whether bacterial activity could also apply to a Mesozoic sequence.

The Recent biofilm on the shell of *Montacuta ferruginosa* is a structured microbial mat showing three separate layers. The most abundant micro-organisms in the biofilm are filamentous bacteria related to Beggiatoaceae. The origin of the red matrix of the Paleozoic series is also related to bacterial constructions. Scanning microscope observations show that filamentous bacteria (also related to Beggiatoaceae) associated with coccoid bacteria are predominant in the red micrites (see for example Mamet et al., 1997; Préat et al., 1999b). Sedimentological conditions as well as iron (bio)mineralization processes are discussed in these papers (see Ehrlich, 1990 for a discussion). Independent of the age, the depositional setting is similar, whether the sedimentary bodies are stratiform (Mamet and Boulvain, 1991; Mamet et al., 1997; Préat et al., 1999a,b) or mud mounds (Boulvain, 1993). The suggested environment is relatively 'deep', fifty to a hundred meters, in quiet marine waters, well below the fair-weather wave base, i.e. close or below the storm wave base and below the photic zone. This suggests anoxic to dysaerobic conditions, where iron (and manganese) is in a soluble reduced state.

The present paper shows that microbes could play a similar role in the formation of various red nodular organic structures and in the early diagenesis of the studied Jurassic sediments in Normandy. It also highlights the sedimentological conditions assuming that condensation is important, creating microaerophilic environments that enhance the biological Fe oxidation mechanisms. Finally, this article indicates that processes related to the activities of microbial communities are applicable to a red condensed Mesozoic carbonate sequence, as previously shown for its Paleozoic counterparts.

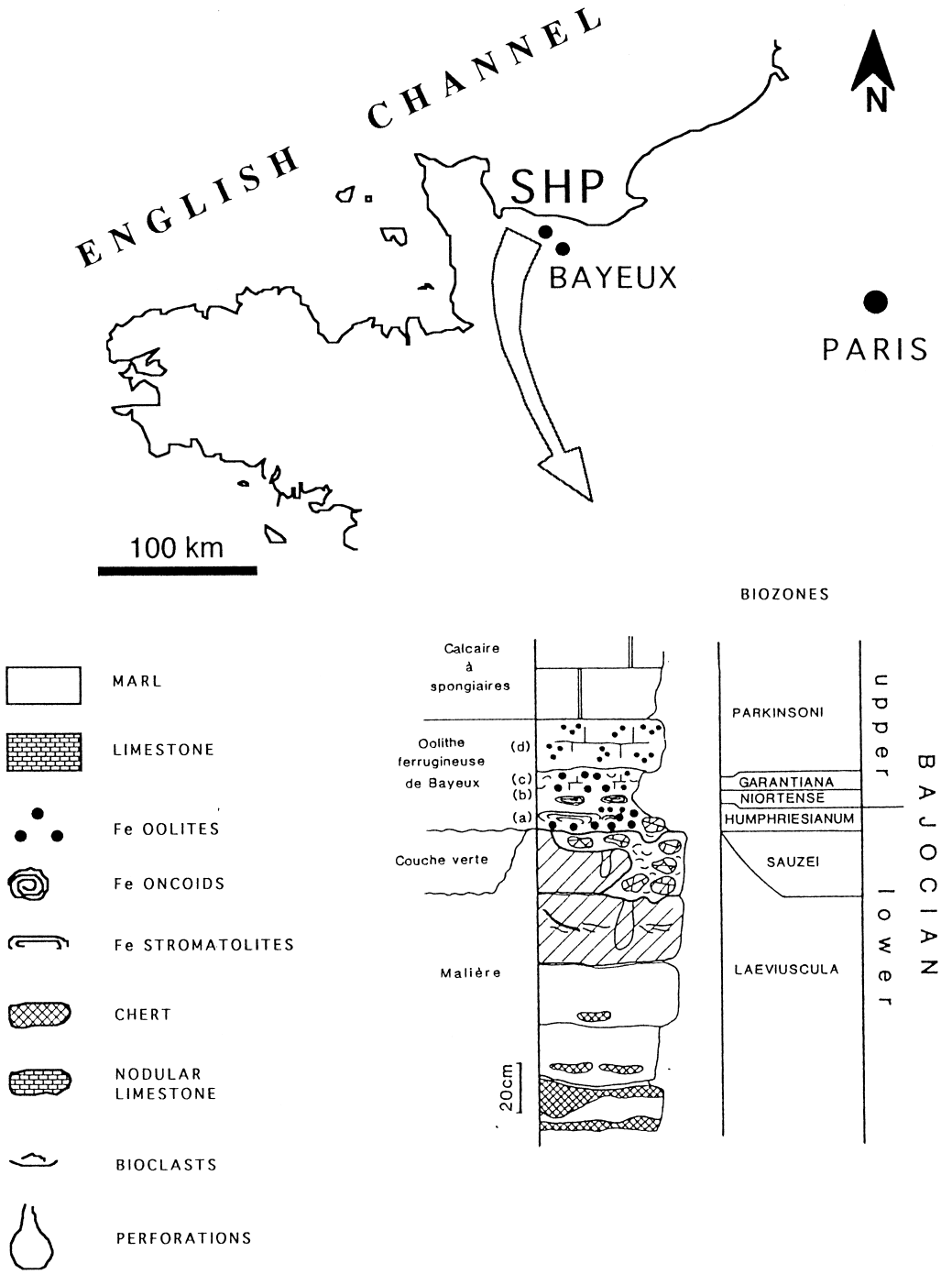

Fig. 1. Geographical location of the stratotype of Sainte-Honorine-des-Pertes (SHP), lithologic log and stratigraphic interpretation based on ammonite zonation (after Rioult et al. (1991)). The Oolithe ferrugineuse de Bayeux Formation is composed of beds a, b, c and d (see text).

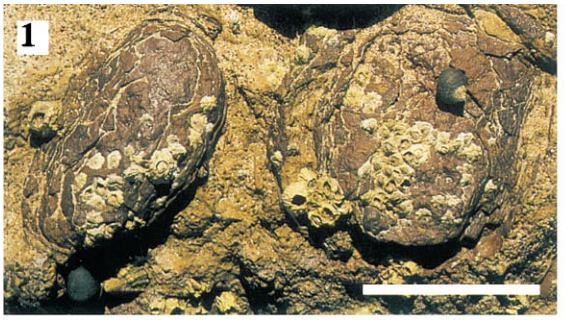
1


2


3

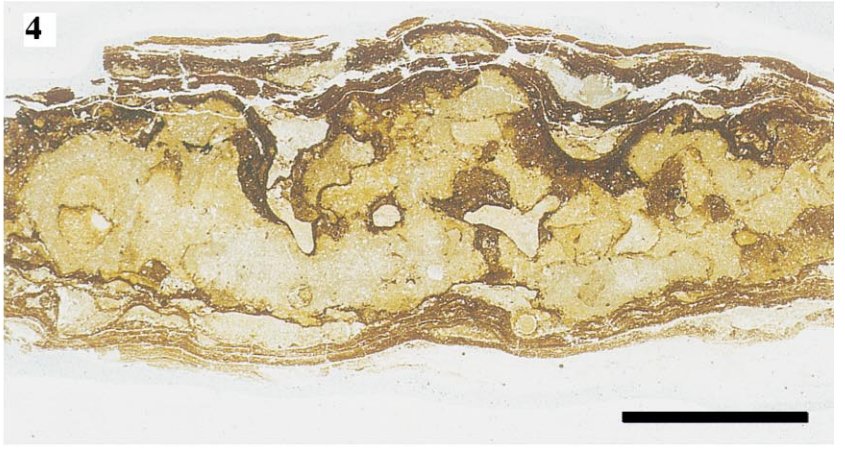
4


5

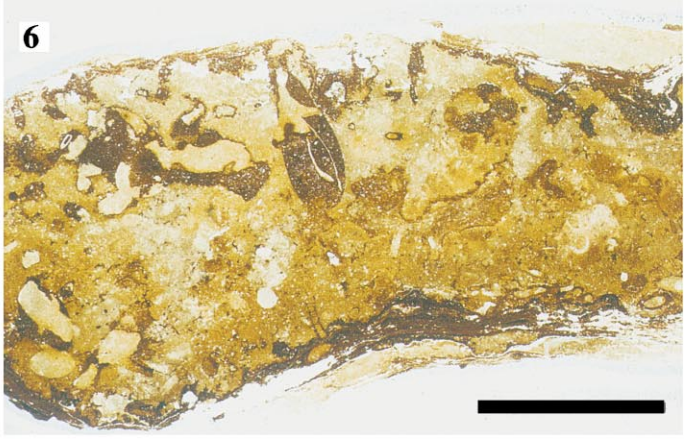
6

2. Jurassic facies and Fe oxide deposits

2.1. Macroscopic description

The Oolithe ferrugineuse de Bayeux (Lower/Upper Bajocian) contains four beds (Rioult et al., 1991) (Fig. 1):

- Bed (a) or 'Conglomerate of Bayeux' (0.05–0.25 m) is composed of ferruginous oncoids (Plate 1, 1–6) with nuclei derived from pebbles or fossil casts reworked from the underlying 'Couche Verte' (0–0.30 m), the top of the Malière (7 m) Formation. Three successive levels are observed: (a1) a basal discontinuous horizon with pebble-sized ferruginous oncoids, (a2) a middle level composed of heterometric (1–10 cm in diameter) ferruginous oncoids, and (a3) an upper horizon composed of a ferruginous stromatolite pavement (up to 10 cm thick);
- The base of bed (b) (0–0.15 m) is a poorly sorted dull oolite with bioclasts. It grades upwards to well-sorted shiny ferruginous ooids with calcitic mollusks;
- Bed (c) (0–0.1 m) is composed of iron ooids in a biomicritic matrix similar to that of bed (b). The number of the ferruginous ooids decreases from beds (b) to (c), and bioclasts are often concentrated in the lower and upper parts. Pavia (1994) reports numerous reworked mollusk fauna and recognizes five ammonoid taphorecords from the nearby Sully sequence.
- Bed (d) is the thickest (maximum 0.3 m) and shows a patchy distribution of ferruginous ooids, because of intense bioturbation. A few whitish phyllitic (Rioult, 1964) and pyritic ooids are mixed with the ferruginous ooids. The muddy calcareous matrix is more abundant than below. The top of bed (d) is cut by a planar surface.

Fernandez–Lopez (1991) and Pavia (1994) report four chrons from the geochronologic scale *Humphriesianum* to *Parkinsoni*.

According to Rioult et al. (1991), the formation encompasses two ammonite zones and one subzone and the sedimentation rate was very low (0.25 m/My). In this context, bed (a) represents a condensed section developed at a time of terrigeneous sediment starvation on the shelf. Hydrodynamic variations are recorded in the lower and middle oncoid horizons. A biostratigraphical gap (*Banskii* subzone and base of the *Polygyralis* subzone) separates beds (a) and (b).

Rioult et al. (1991) suggest that the ferruginous oncoids and stromatolites were built by the activity of cyanobacteria in the photic zone. Biological processes were effectively predominant in the formation of the observed organic structures, but they were related to the activity of filamentous fungi and bacteria in the much deeper dysphotic zone.

2.2. Microfacies and ferruginous structures

Samples and ferruginous 'nodules' come from all four beds of the Bayeux Oolithe. In thin sections, three microfacies (MF1 to MF3) are recognized: MF1, oncoidal floatstone and rudstone associated

Plate 1. 1,2. Rounded ferruginous brown oncoids exposed on the beach of Sainte-Honorine-des-Pertes. ULB, photographs Préat D10/1 et D10/2, bed (a) in Rioult et al. (1991), scale bar 5 cm (figure 1) and 1 cm (figure 2). The oncoidal nucleus is a small ammonite (figure 2). 3. Ferruginous oncoid nodule in a bioclastic (sponges, ostracods, see Plate 5, 1–3) mudstone/wackestone. Nucleus, a ferruginous cortical layer (middle bottom) with bryozoans and serpulids. Numerous thin, regular and irregular ferruginous crusts and a few trapped ferruginous ooids (central part). The vertical right part of the photograph is the stratigraphic base. See Plate 5, 1–3) for detailed structure of the oncoid. Sample Shp7, photograph Préat D10/5, bed (a) in Rioult et al. (1991), scale bar 1 cm. 4. Ferruginous oncoid with strong polyphased burrowing and internal hardground erosional surfaces (see the bottom). Nucleus composed of a fine bioclastic (echinoderms, planktonic foraminifers…) silty sponge packstone. Ferruginous cortex contains various bacterial filament types (see Sample Shp6, Plate 6, 1, 10–12). The base of the photograph is the stratigraphic base. Sample Shp2, photograph Préat D10/3, bed (a) in Rioult et al. (1991), scale bar 1 cm. 5. Complex ferruginous oncoids with corroded cortical layer at the bottom (see also Plate 5, 4), ferruginous stromatolitic crusts and irregular lateral dark ferruginous cortical layer at the top (see also Plate 5, 5). Slightly asymmetrical ferruginization on the lower part of the upper oncoid (Plate 5, 5). The base of the photograph is the stratigraphic base. Sample Shp1, photograph Préat D10/7, bed (a) in Rioult et al. (1991), scale bar 500 μm. 6. Strongly perforated ferruginous oncoid. Partly ferruginized nucleus with microbioclastic sponge wackestone, small planktonic foraminifers and pelecypods (see Plate 2 , 3). See also Plate 2, 3 and Plate 3, 1 for a detailed description. The base of the photograph is the stratigraphic base. Sample Shp5, photograph Préat D10/9, bed (a) in Rioult et al. (1991), scale bar 1 cm.

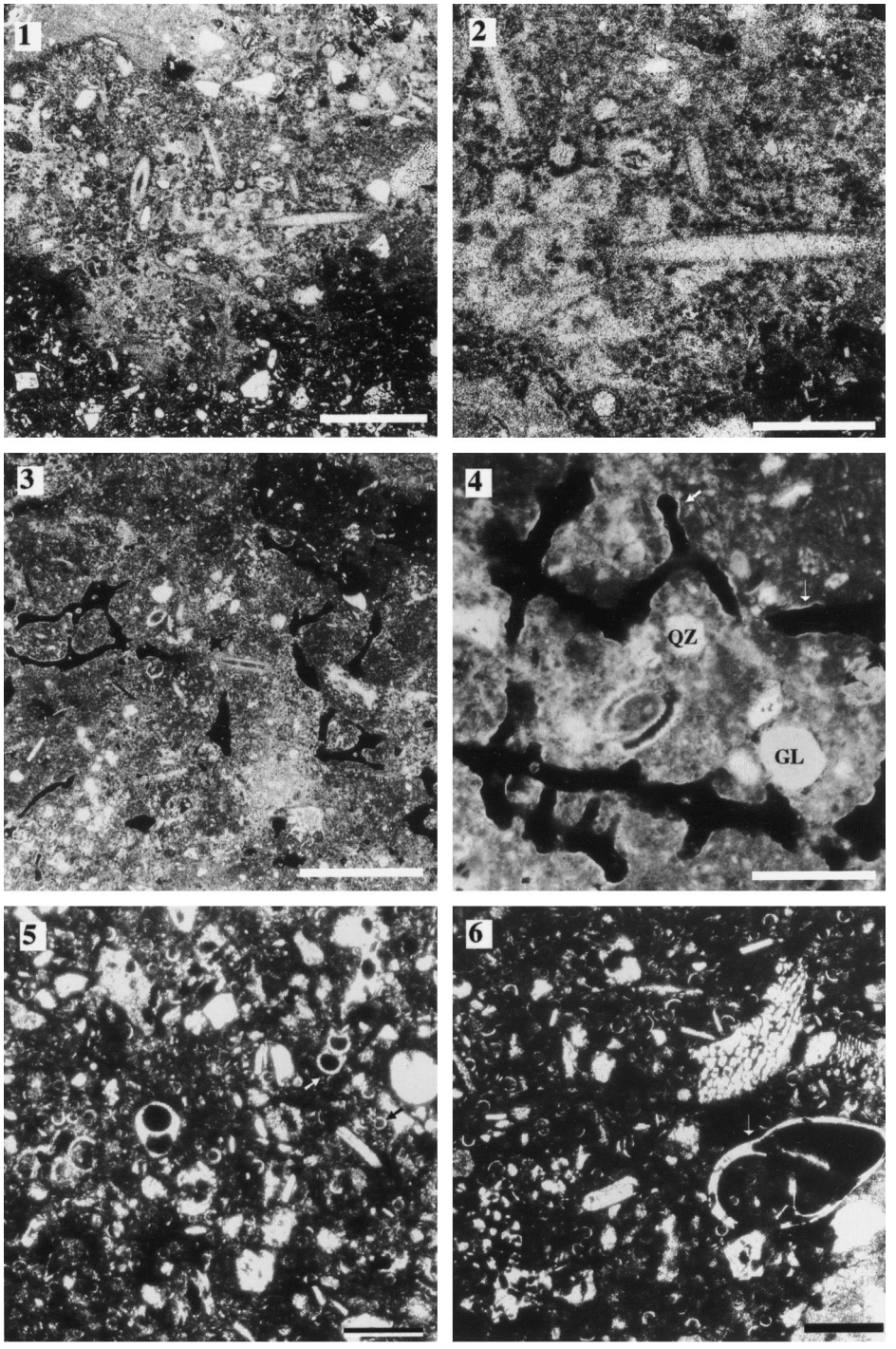
1
2
3
4
QZ
GL
5
6

with bed (a); MF2, ooidal packstone observed in beds (b) and (c); MF3, silty burrowed wackestone/packstone of bed (d). Due to the abundance of ferruginous microorganisms in bed (a), we will concentrate on the ferruginous oncoids of that level.

2.2.1. Microfacies 1

Ferruginous oncoids of MF1 are cobble-sized, with their long axes parallel to the bedding (Plate 1,1). The cortex, up to 2 cm thick, is asymmetric, the larger side facing downwards. Laminations consist of thin alternations of dark- and light-coloured hematite, each couplet averaging a thickness of <300 μm. The layers show both continuous and discontinuous bands. In addition, the cortex is composed of calcareous encrusting fauna (serpulid worms, Plate 3, 2, abraded or microbored sponges and bryozoans) and trapped bioclasts (foraminifers, mollusks, echinoderms). It sometimes contains a few glauconite grains (Plate 5, 4). Successive hematite laminations (cortex) are interstratified with local lenses (0.5–1 mm thick, 2–5 mm long) of calcite crystals and fine micrite, the latter being rich in sponge spicules. The calcite crystals contain abundant and diversified Fe microbial filaments (see below). The nucleus is generally shelly (ammonoid fragment) or lithoclastic (sponge bioclastic packstone). It consists of a greyish to brownish bioclastic silty sponge wackestone/packstone with mollusks (bivalves and ammonites), crinoids, ostracods, small planktonic foraminifers (mainly *Protoglobigerina*) and a few glauconite grains (up to 100 μm: Plate 2, 1–6; Plate 3, 3). The matrix is strongly bioturbated and consists of multiple generations of firm-ground millimetric to centimetric-sized *Chondrites* burrows, wholly or partly filled with bioclastic sponge wackestone/packstone (Plate 1, 4, 6; Plate 2, 1–3; Plate 3, 1, 3, 5). Burrows have few vertical elements and abundant horizontal or gently inclined tunnels. They are circular in cross section, of constant diameter (between 1 to 3 mm) and have smooth walls. Branching is regular. Three episodes of burrowing are present and distinguishable by the color of the infillings. Burrows of phase 1 are filled with a dark microbioclastic wackestone. They are cut by burrows of phase 2 (grey mudstone/wackestone rich in sponge spicules, Plate 1, 4, 6 and Plate 3, 1) and finally by burrows of phase 3 (brownish to reddish bioclastic wackestone). The perforated MF1 matrix and bioclasts (mollusks, sponge spicules, echinoderms) are ferruginized (Plate 4, 1–6). Matrix perforations are well defined (1 cm deep and 0.3 cm in diameter) or diffuse (mm to cm-sized) and may be infilled by at least three types of sediment (Plate 1, 6; Plate 3, 1, 5).

Ferruginous laminated crusts (up to 1.5 cm thick) inside the sediment form delicate interfingerings or lateral expansions of the oncoidal cortex (Plate 1, 3, 5; Plate 5, 3). Numerous thin ferruginous hardgrounds with Fe microbial filaments and small- to medium-sized Fe microstromatolites (up to 5 mm) are associated with the two crust types (cortex and 'expansional') and form a second type of Fe layered oncoid–stromatolitic carbonate nodule (Plate 1, 3; Plate 5, 1, 2). These nodules are commonly ovoidal in shape, their sizes ranging from a few mm up to 4 cm (or more as illustrated by Fürsich, 1971, p.325). The sediment is a sponge wackestone/bafflestone (Plate 5, 3) and trapped particles consist mainly of small planktonic foraminifers and various perforated bioclasts. Serpulid bafflestones are frequently associated with the stromatolitic layering (Plate 5, 1, 2).

Plate 2. All figures are from the nucleus of ferruginous oncoids. 1, 2. Bioturbated, microbioclastic (ferruginous . echinoderms, small foraminifers and minute molluskan fragments) wackestone/packstone with silty quartz grains. Dark brown matrix comparable to that of figures 5 and 6 (Plate 1). Burrow filled by a greyish spicule sponge packstone with a ferruginous micropeloidal texture and a very fine-grained calcitic microspar (figure 2). Matrix also contains a few silty quartz and glauconite grains. ULB, photograph Préat 51/21 Sample Shp3, bed (a) in Rioult et al. (1991), scale bar 500 μm (figure 1) and 250 μm (figure 2). 3,4. Bioturbated microbioclastic (pelecypods, altered echinoderms and small planktonic foraminifers) sponge wackestone with silty quartz grains. Ferruginized sponge network (figure 4) with a thin discontinuous calcitic coating (white lamina) (arrows). Silty quartz and small glauconite grains (figure 4). Figure 3 shows the grey dark matrix of the lower part of Plate 1, 6. ULB, photograph Préat 53/20 Sample Shp5, bed (a) in Rioult et al. (1991), scale bar 250 μm (figure 3, 4) and ULB, photograph Préat 53/10 Sample Shp8, bed (a) in Rioult et al. (1991). 5. Bioclastic (small planktonic foraminifers [see arrow] and altered echinoderms) packstone. Foraminifers completely filled by massive hematite. ULB, photograph Préat 51/18 Sample Shp3, bed (a) in Rioult et al. (1991), scale bar 100 μm. 6. Bioclastic (planktonic foraminifers, altered echinoderms and pelecypods) wackestone. Foraminifer filled by massive hematite. Ferruginous micrite underlines the pitting of the echinoderm plates. Ferruginous hair-like perforations in foraminiferal wall. ULB, photograph Préat 51/14 Sample Shp3, bed (a) in Rioult et al. (1991), scale bar 100 μm.

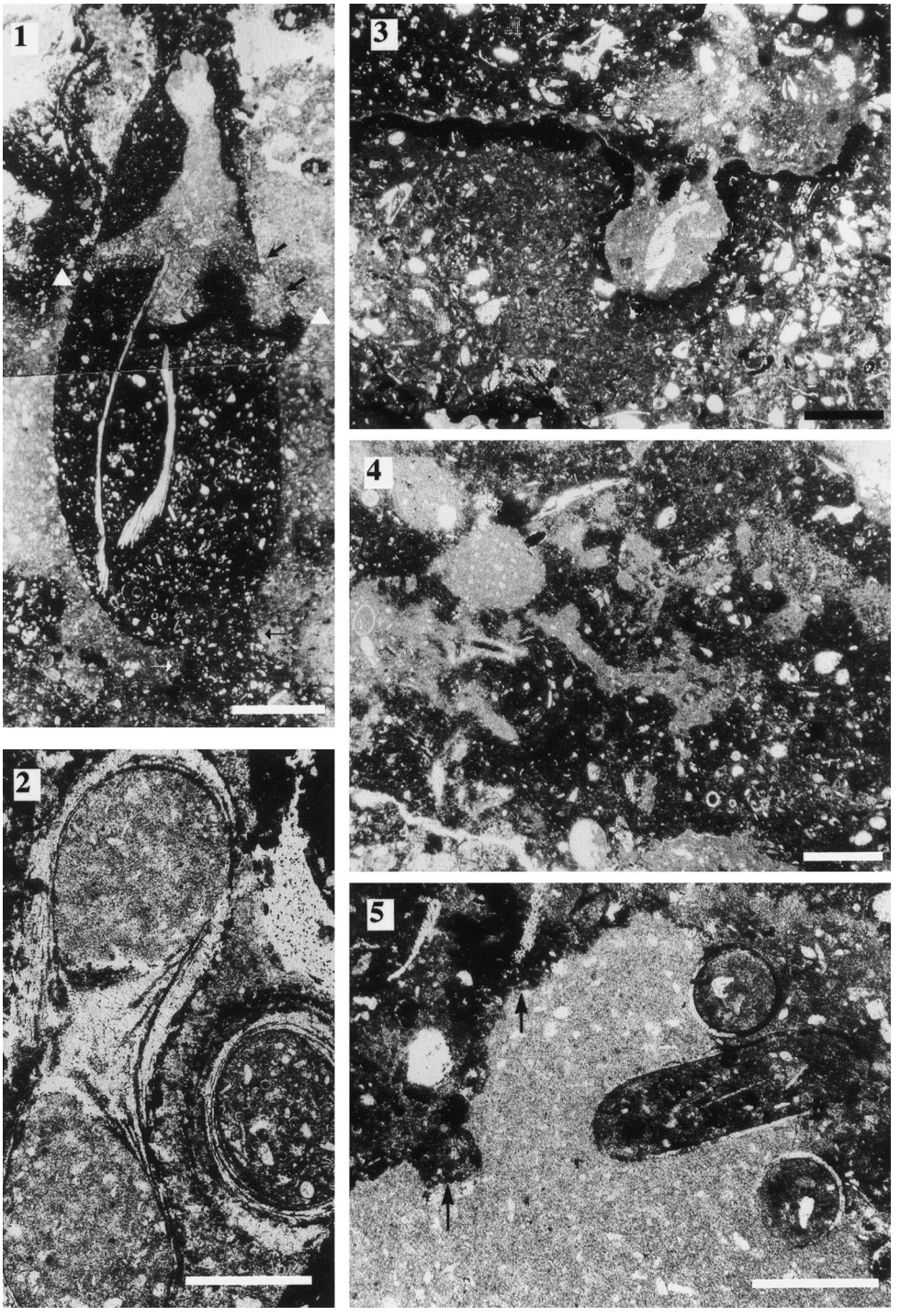
1
2
3
4
5

They are similar to those of the oncoid cortical laminations. Perforations are filled with sponge spicule wackestone/packstone that occasionally contain small Fe ooids. A few calcite dissolution cavities are present. No fenestral fabric has been observed. The thin oncoid–stromatolitic layering occasionally presents an asymmetrical development, being thicker at its base (Plate 1, 5). Hardgrounds are also free in the matrix, i.e. without any relation with the nodules, and occur in all directions (Plate 3, 3). They are irregular, continuous or discontinuous. Numerous Fe filamentous microorganisms are associated. In complex hardgrounds, the crust forms an in situ 'conglomerate' of poorly sorted subrounded fragments that suggest corrosion. Microstromatolites are also observed in the matrix or on the shell walls.

2.2.2. Microfacies 2

MF2 is an ooid bioclastic packstone that contains centimetric-sized sponge microbreccia of the floatstone and rudstone microfacies (MF1). Microbreccia are ferruginized, strongly perforated and show asymmetric encrustations by Fe microstromatolites. Ferruginous ooids are millimetric in size, moderately to well-sorted with a grain size ranging from 0.6 to 1.4 mm. They are sometimes polyphased and encrusted by Fe microstromatolites, which cement several ooids. Their nuclei are generally composed of a fine-grained microbioclastic wackestone/packstone. They rarely contain glauconite grains. A few ooids are broken. The bioclasts consist mostly of large bivalves, associated with a few belemnites, which are strongly bored and ferruginized (Plate 4, 5, 6). The micrite matrix is a heavily bioturbated non-ferruginous wackestone. Galleries are filled by a sponge clotted ferruginous peloidal packstone rich in crinoids and bioclasts (mollusks, ostracods). Burrows are invaded by ferruginous mats and microstromatolites that bind the elements including ferruginous ooids, which were incorporated or trapped in the galleries. The wackestone matrix contains a few silty quartz grains. Skeletal cavities, perforated cavities of the shells (mainly the mollusks), sheltered cavities below the bioclasts ('umbrella'), may represent geopetal infillings. Despite the different orientations of the shells, geopetal infillings are parallel between them suggesting that the perforations are in situ and took place inside the sediment. They are accompanied by various Fe microorganisms.

This facies is quite similar to the 'ooidal ironstones' of Kimberley (1978) and Young (1989) and refers here to lithology containing >5% ferruginous ooids.

2.2.3. Microfacies 3

MF3 is a silty sponge burrowed wackestone/packstone that contains various mollusk bioclasts. Ferruginization processes are absent.

2.2.4. Ferruginous structures

Ferruginous structures are numerous as the hematite

Plate 3. Except figure 2, all figures are from the nucleus of ferruginous oncoids. 1. Millimetric (9 × 2.5 mm) perforation filled by a iron-encrusted pelecypod shell and small planktonic foraminiferal wackestone that contains silty quartz grains, small ostracods and altered echinoderms. Perforated sediment is a microbioclastic wackestone rich in small planktonic foraminifers. The sediment filling the perforation is bioturbated at its base, the bioturbation affecting original sediment (arrow). At the top (above the white triangles) a discrete burrow (*Chondrites* isp.) is filled by a greyish microbioclastic wackestone with small glauconite grains. The burrow also affects the host sediment. The contact between the dark sediment filling the perforation and the grey sediment of the burrow is underlined by a ferruginous layer (between the two white triangles) similar to that of the oncoid cortex. See also Plate 1, 6 for the general view. Photographs Préat 51/15-16-17 Sample Shp5, bed (a) in Rioult et al. (1991), scale bar 1 mm. 2. Serpulid tubes (bafflestone) encrusted by the ferruginous cortical layers of the oncoid of sample Shp3 (see Plate 2, 1, 2, 5, 6). Tubes filled by a microbioclastic (planktonic foraminifers and pelecypods) wackestone-packstone with a few silty quartz grains. The wall of the serpulids are partly ferruginized. ULB photograph Préat 51/20 Sample Shp3, bed (a) in Rioult et al. (1991), scale bar 250 μm. 3. Irregular, perforated ferruginous hardground in a bioturbated microbioclastic (altered echinoderms and perforated mollusks) wackestone containing silty quartzose and glauconite grains. Numerous ferruginous microbial filaments are present within the hardground and are similar to those illustrated, Plate 6, 11, 12. ULB, photograph Préat 51/12 Sample Shp8, bed (a) in Rioult et al. (1991), scale bar 500 μm. 4. Strongly burrowed (*Chondrites* isp.) dark microbioclastic (small planktonic foraminifers, and pelecypods) wackestone. Burrows filled by greyish microbioclastic mudstone/wackestone. ULB, photograph Préat 51/26 Sample Shp3, bed (a) in Rioult et al. (1991), scale bar 500 μm. 5. Non-ferruginous microbioclastic (echinoderms, pelecypods) greyish wackestone filling a burrow (just a part of it is visible). This is cut by a very irregular ferruginous hardground showing corrosion (arrow) and encrustation by small serpulid tubes with partly ferruginized walls. Dark sediment associated with the hardground is a microbioclastic (planktonic foraminifers and altered echinoderms) wackestone with subrounded silty quartz grains. ULB, photograph Préat 51/25 Sample Shp3, bed (a) in Rioult et al. (1991), scale bar 250 μm (arrows).

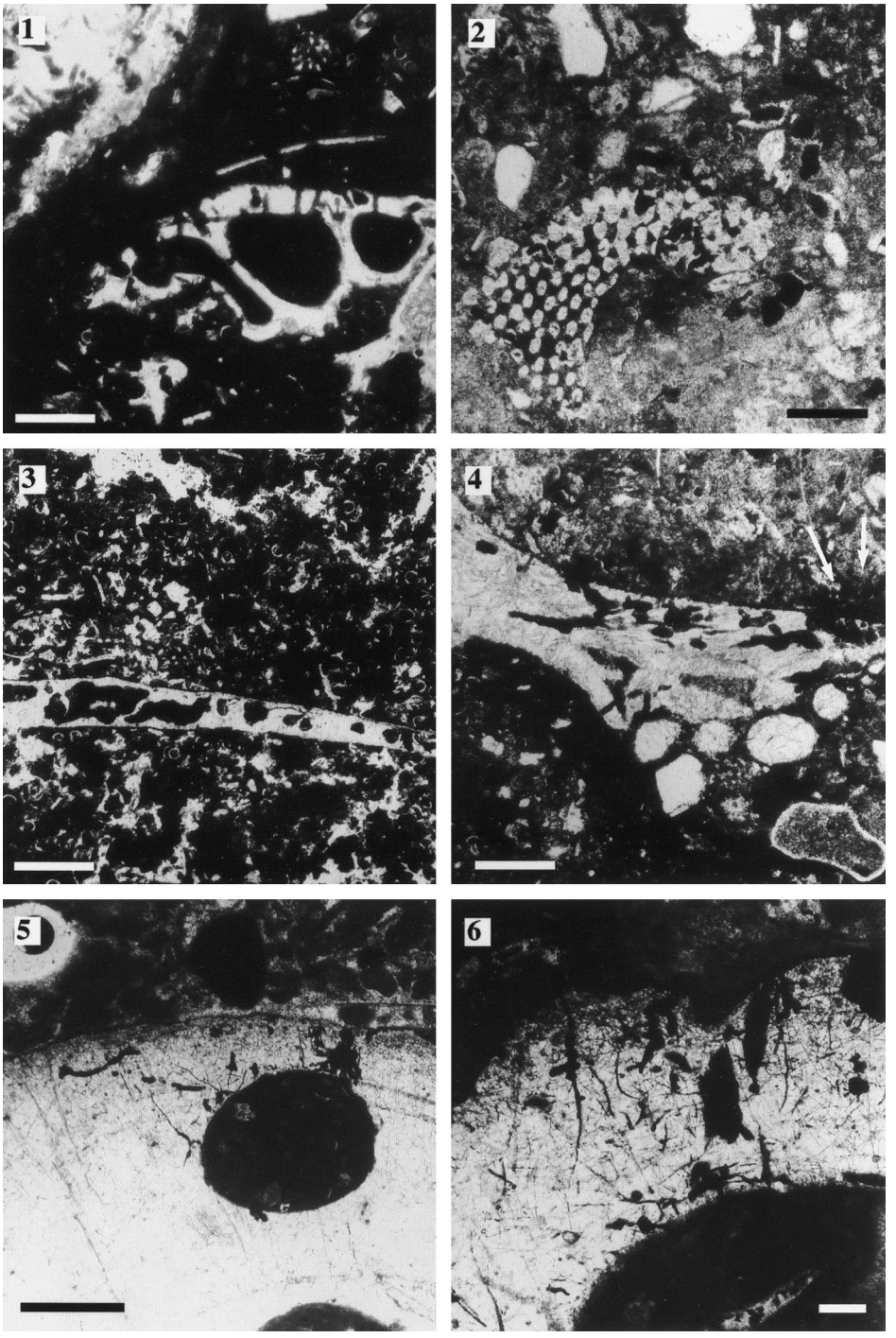
1
2
3
4
5
6

staining follows many patterns. Among the more widespread are perforations infillings (Plate 3, 1, 2, 5) with endolithic microorganisms (Plate 4, 1, 3–6), microstromatolites (Plate 5, 1–3), oncoids, ooids, blisters, coatings and hardgrounds (Plate 1, 3–6; Plate 3, 3). These structures are often associated and none are mutually exclusive. They present filaments (Plates 6 and 7) of different sizes and shapes in the micrite matrix, in the calcite walls of various organisms, in the calcite crystals associated with the Fe cortical laminations, in the perforations, in the burrows, in the hardgrounds and in microstromatolites. Similar structures have been described in the Paleozoic by Mamet et al. (1997) and Préat et al. (1998, 1999a,b).

2.3. Depositional environment. Early diagenetic evolution

One of the characteristic features of the series is the strong condensation. Frequent sea-level variations provoked disequilibria in the environmental conditions. Comparison with other ferruginous oncoid and ooid genesis (see for example Burkhalter, 1995) suggests episodes of slow deposition to non-deposition and open marine environment.

Thin-section analysis of beds (a) and (b) indicates evolution in five phases:

1. Sedimentation was in very quiet environment, below the photic zone and below (bed a) or near (bed b) the storm wave base. Bed (a) belongs to a distal carbonate ramp, its lower part characterized by hemipelagic sedimentation indicated by planktonic foraminifers. Inferred depth is about 100 m. Free oxygen concentration was very low. Dysaerobic conditions are indicated by weak bioturbation and scarcity of benthic macrofauna. The brownish microbioclastic silty sponge mud (wackestone: Plate 2, 1–6; Plate 3, 4) contains reworked rolled and worn ammonites and lithoclasts of the underlying Malière Formation.
2. During early lithification, the mud was perforated and burrowed by *Chondrites* isp. (and/or *Thalassinoides* isp. *sensu*; Fürsich, 1971) recording colonization of a progressively firmer ground (Plate 1, 4, 6). *Chondrites* isp. burrows are filled by bioclastic sponge wackestone-packstone. Several discrete forms of well-defined burrows suggest a network development (Plate 3, 4, 5). These ichnofossils occupy the deepest tiers (Lockair and Savrda, 1998) below the surface in dysaerobic bottom waters of low-energy basinal environments (Bromley, 1990; Fürsich, 1998). The bioturbation densities are around 50% (Plate 1, 4, 6; Plate 3, 4). Burrowers are restricted to *Chondrites* isp. indicating a low diversity ichnofacies and inhospitable zones (Bromley, 1990). Cross-cutting relationships indicate that at least three episodes of burrowing took place. *Thalassinoides* isp. have been reported by Fürsich (1971) and could indicate non-sedimentation periods.
3. Fe cortices of the oncoids formed around nuclei, and ferruginous laminated crusts developed inside the sediment as lateral expansions of the oncoid cortex (Plate 1, 3, 5; Plate 4, 1; Plate 5, 4, 5).

Plate 4. Figures. 2, 3 and 4 are from the nuclei of ferruginous oncoids. 1. Dark ferruginous cortex of a oncoid with perforated gastropod shell (center of the figure), molluskan shell fragments (upper left corner, above and below the gastropod) and altered echinoderm plate (upper part). Presence of quartz grain (the middle part, top of figure). Gastropod wall shows endolithic perforations with coarse ferruginous filaments orthogonal or parallel to the borders. ULB, photograph Préat 52/11 Sample Shp3, bed (a) in Rioult et al. (1991), scale bar 100 μm. 2. Bioclastic (altered echinoderm plate, small planktonic foraminifers, ostracods) wackestone with subrounded silty quartz grains (upper part of the figure). ULB, photograph Préat 51/34 Sample Shp3, bed (a) in Rioult et al. (1991), scale bar 100 μm. 3. Perforated pelecypod shell in a microbioclastic (mollusks, small planktonic foraminifers, ostracods) ferruginous micrite. Hematite-filled sponge perforations in the pelecypod and ferruginous filaments between the perforations. ULB, photograph Préat 52/4 Sample Shp3, bed (a) in Rioult et al. (1991), scale bar 100 μm. 4. Perforated pelecypod shell in a bioclastic ferruginous micrite with silty quartz grain and small planktonic foraminifers. Perforations filled by hematite. Ferruginous filaments along the calcitic fibrous microstructure. Three perforations are penetrating the inside wall from the sediment (arrows). ULB, photograph Préat 51/35 Sample Shp3, bed (a) in Rioult et al. (1991), scale bar 100 μm. 5, 6. Perforated belemnite in an ooid and oncoid rudstone. Perforations are circular, of constant diameter (2 mm) and filled by bioclastic (perforated echinoderms and mollusks, figure 6) wackestone. Numerous long microbial ferruginous filaments in the wall are located in the outer part of the belemnite (no filaments in the central perforation, bottom of figure 5). ULB, photograph Préat 53/34 Sample Shp12 (figure 5) and photograph 53/36 Sample Shp12 (figure 6), bed (a) in Rioult et al. (1991), scale bar 500 μm (figure 5) and 100 μm (figure 6).

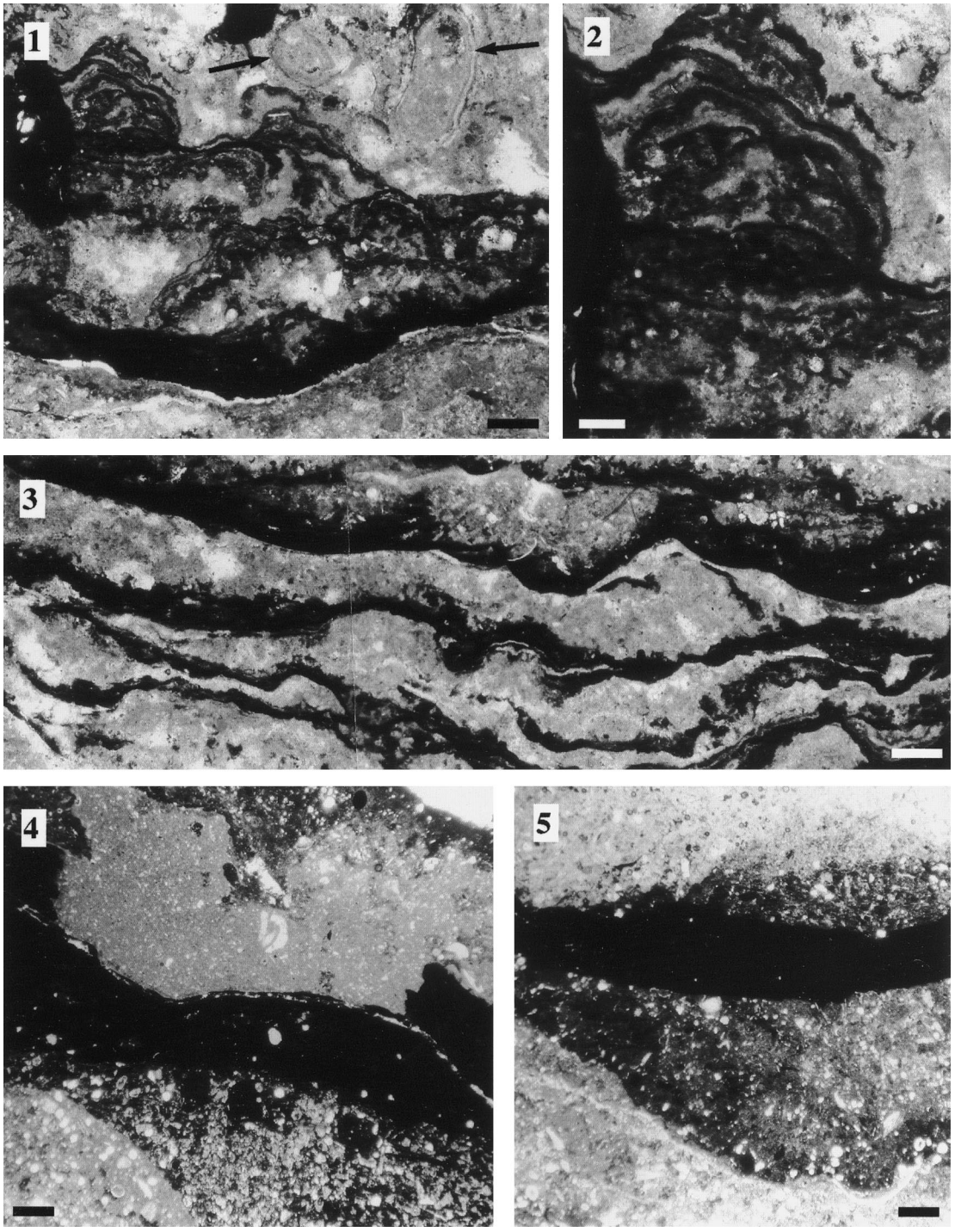
1
2
3
4
5

The beginning of these cortical and crustal formations was accompanied by an erosive and corrosive phase that affected the previous structures (sediments, burrows, perforations and bioclasts; Plate 1, 6) and the ferruginous cortex itself (Plate 3, 5; Plate 5, 4). The fauna colonized small gloomy cavities and crevices. Iron layering occurs on the gloomy undersides of the nuclei (Plate 5, 5), within the sediment as expansions of the cortex of the oncoids (Plate 5, 1, 2), or grows following a centripetal direction in the oncoid (Plate 5, 3). This suggests an in situ development of the non-photosynthetic filamentous microorganisms. The environment was quiet since 'expansional layering' is delicate and in close interfingering with the oncoid cortex. Numerous thin to thick Fe hardgrounds developed and were coeval with the oncoid formation. Fe microstromatolites and various ferruginous microbial filaments grew inside the sediment, while the hardgrounds develop in all directions (Plates 6 and 7).

4. After a probable phase of sea-level lowering (top of bed (a)), MF2 was formed by mixing corroded MF1 microbreccias (mainly altered ferruginous oncoids) and MF1 perforated bioclasts (ammonites, belemnites: Plate 4, 5, 6) with ferruginous ooids and large shallow perforated bioclasts (beds (b) and (c)). The energy level was higher. The perforations of the MF1 bioclasts show abundant long filamentous microorganisms, unlike those of the MF2. The MF2 matrix is greyish and in situ ferruginization is episodic and associated with local burrowing of the matrix and perforation of the shells. The bottom waters were now oxic with occasional local dysaerobic microenvironments (burrows and perforations).
5. Oxygen levels continued to increase and the environment was colonized by sponges of the MF3 (bed (c)). Ferruginization processes were not observed.

3. Microbial assemblages in the Fe precipitates

An examination of polished sections under the light microscope and the SEM, and of acid-leached sections under the SEM, indicates seven types of microfossils: filaments (five morphotypes), spheroidal bodies and stalked bodies. These microorganisms are observed in all the ferruginous coatings, endolithes, in many calcite crystals, in microstromatolites and in various cavities.

Filaments show no cells and are heavily encrusted by iron minerals.

Type 1 filaments (Plate 6, 1) are 0.2–0.7 μm wide and about 10 μm long.

Type 2 filaments (Plate 6, 1–8, 9) are 1.3–3.5 μm wide and more than 100 μm long.

Type 3 filaments (Plate 6, 7, 10–12) are 5.5–8.5 μm wide and up to 180 μm long.

Type 4 filaments (Plate 6, 8, 9) are 15–18 μm wide and about 420 μm long; these filaments are not abundant.

Type 5 filaments (Plate 7, 1–6) are 33–60 μm wide. These filaments branch regularly to form net-like structures, or three-dimensional networks.

Plate 5. 1, 2. Microstromatolitic ferruginous crust in a bioclastic (sponges, ostracods, see figure 3) mudstone/wackestone (from the oncoidal nodule, Plate 1, 3). Numerous ferruginous filaments are associated with the nodule and similar to those illustrated on Plate 7, 10–12. Encrusted serpulid tubes (arrows, top of figure 1) form a bafflestone. See Plate 1, 3 for a general view. ULB, photographs Préat 53/5 (figure 1) and 53/6 (figure 2), Sample Shp7, bed (a) in Rioult et al. (1991), scale bar 250 μm (figure 1) and 100 μm (figure 2). 3. Asymmetrical ferruginous hardground crusts in the same oncoid as figures 1 and 2 (the centre of the oncoid is towards the top of figure 3) with numerous ferruginous filaments growing towards the inner part of the oncoid (Plate 7, 10–12). The matrix is a bioclastic (sponges, ostracods) mudstone/wackestone. See also Plate 1, 3. ULB, photographs Préat 53/3-4 Sample Shp7, bed (a) in Rioult et al. (1991), scale bar 250 μm. 4. Corroded and perforated ferruginous dark layer. Accretion of 5–10 μm thick laminae, rich in filamentous microorganisms (Plate 6). The crust contains a glauconite grain. The core (bottom of the figure) is a perforated bioclast. Perforation of the crust and of the overlying sediment (dark ferruginous bioclastic wackestone, top of the figure) filled by a greyish microbioclastic sponge mudstone/wackestone. The base of the photograph is the stratigraphic base. See also Plate 1, 5 for the general view. ULB, photograph Préat 53/30 Sample Shp1, bed (a) in Rioult et al. (1991), scale bar 500 μm. 5. Dark ferruginous cortex around a lithoclast (top of the figure) in a greyish microbioclastic sponge bafflestone. Incomplete ferruginization occurs from the cortex, inside the oncoid (in the lithoclastic core) and outside in the sediment. Ferruginization is thicker under the oncoid. The base of the photograph is the stratigraphic base. See also Plate 1, 5 for the general view. ULB, photograph Préat 53/28 Sample Shp1, bed (a) in Rioult et al. (1991), scale bar 500 μm.

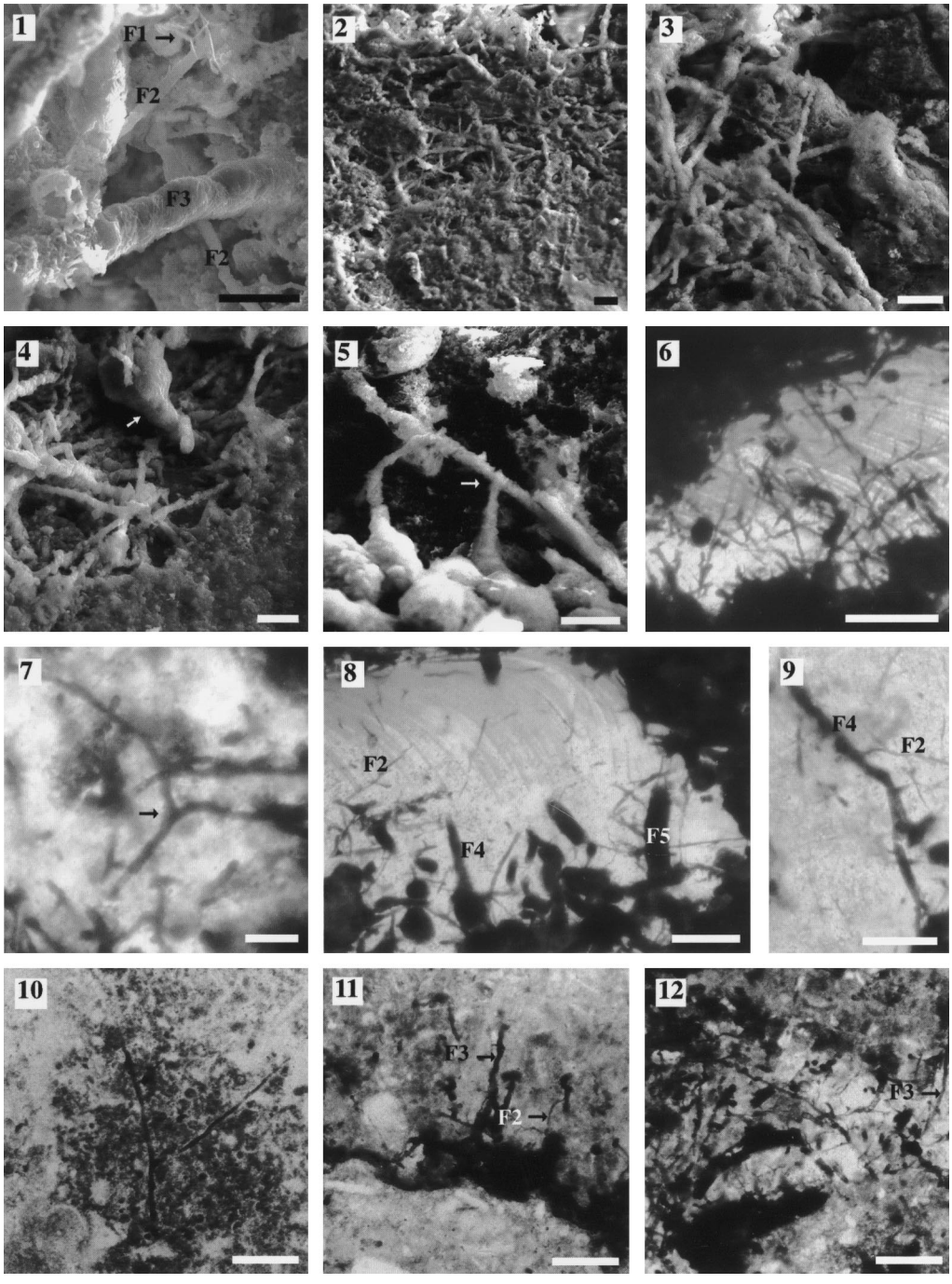
1
F1
F2
F3
F2
2
3
4
5
6
7
8
F2
F4
F5
9
F4
F2
10
11
F3
F2
12
F3

Segments are about 150 μm long. The surface of these filaments is riddled with 2–4 μm holes and are coated by thin and regular lamellar or 'specular' hematite crystals (Plate 7, 5).

Spheroidal bodies (Plate 7, 7–9) are 13–25 μm wide. They present a rough surface, are encased in mineral deposits and frequently associated with type 2 filaments (Plate 7, 9).

Stalked bodies (Plate 6, 4; Plate 7, 6) are 30–54 μm wide and 30–120 μm long. The stalk is 5–12 μm wide. These structures are not abundant. In polished sections, large stalked bodies contain 4–5 spheroidal inclusions (about 18 μm wide) and are associated with type 5 filaments.

Microstromatolites (Plate 5, 1, 2; Plate 7, 10–12), observed in polished sections, are frequently associated with filamentous microfossils and hardground crusts (Plate 7, 11).

4. Discussion

4.1. Site of ferruginous microbialite growth

Sediments were deposited in quiet environments, below the photic zone and below (bed (a)) or near (bed (b)) the storm wave base. From the distribution of the numerous ferruginous structures described here, it is possible to make some inferences about the habitat, and therefore controlling environmental factors of the bacteria and fungi. Microbes inhabit the microenvironments on the lower surfaces of the oncoids, they grow centripetally in the oncoid–stromatolite layers and they are associated with delicate expansional cortical crusts derived from oncoids. This indicates that they developed inside the sediments, that they are non-photosynthetic and probably heterotrophic or chemoautotrophic. Free oxygen concentration was very low and dysaerobic conditions prevailed. In these conditions, the stability of the reduced form of iron (Fe^{2+}) is higher.

Oncoids also contain calcareous skeletons of various encrusting organisms. This sessile fauna (serpulids, bryozoans, mollusks…) indicates that oxygen levels changed repeatedly, allowing the temporary development of oxygen gradients in the sediments. Oxygen fluctuations are probably related to sea-level variations. These sessile benthic organisms frequently occur on both sides of elongated nodules, suggesting these nodules were episodically overturned. Grazing organisms could have been responsible for these displacements as observed in equatorial North Pacific (Von Stackelberg, 1987). Growth of manganese nodules are related to the grazing activity of holothurians and fish. The interfingering ferruginous crusts and microbial mats probably stabilized the sediment surface, preventing resuspension of mud or frequent movements of the oncoids (Dahanayake and Krumbein, 1986). This also can explain the asymmetrical microbial growth of the oncoid lower surfaces.

Coeval cementation also occurs during the growth of microbes as indicated by the calcite crystals interlayered in the cortex of the oncoids. Crystals are composed of a single phase and contain remains of microbes that are still connected to the cortical layers. These remains are the same as those observed in mollusks and other bioclasts entrapped in the ferruginous cortex. They correspond to endolithic borings that follow pre-existing calcite and aragonite structures. A similar situation has been reported in large cavities of the Frasnian mud mounds in Belgium (Mamet and Boulvain, 1988). Metric-sized cavities are filled by numerous generations of radiaxal calcite, which were originally filled by bacterial 'spider-webs' on which microstromatolites grew.

Plate 6. Figures 1–9 from sample Shp6, similar to the one illustrated on Plate 1, 2. 1. Type 1 (F1), type 2 (F2), and type 3 (F3) filaments. Acid-leached section, SEM. ULB, Préat shp22(sem), scale bar 10 μm. 2–6. Type 2 filaments. Arrow in figure 4 shows a small stalked body, and arrow in figure 5 shows a dichotomy. Acid-leached sections, SEM (figures 2–5), and polished section (figure 6). Filaments of figure 6 are endolithic (?). ULB, Préat shp42(sem) (figure 2), Préat shp47(sem) (figure 3), Préat shp48(sem) (figure 4), Préat shp35(sem) (figure 5), Préat 45/35 (figure 6). Scale bars 10 μm (figures 2–5) and 50 μm (figure 6). 7. Type 3 filaments (arrow shows a dichotomy). Polished section. ULB, photograph Préat 44/11, scale bar 30 μm. 8, 9. Endolithic (?) type 2 (F2), type 4 (F4), and type 5 filaments (F5). Polished section. ULB, photographs Préat 44/5 (figure 8) and 44/31 (figure 9), scale bars 100 μm. 10–12. Type 2 (F2) and type 3 filaments (F3). Polished sections. ULB, photograph Préat 51/7 Sample Shp3 (figure 10), photograph Préat 52/24 Sample Shp1, (figure 11), photograph Préat 52/22 Sample Shp1 (figure 12). See also Plate 1, 5 for a general view of figures 11 and 12. Scale bars 100 μm.

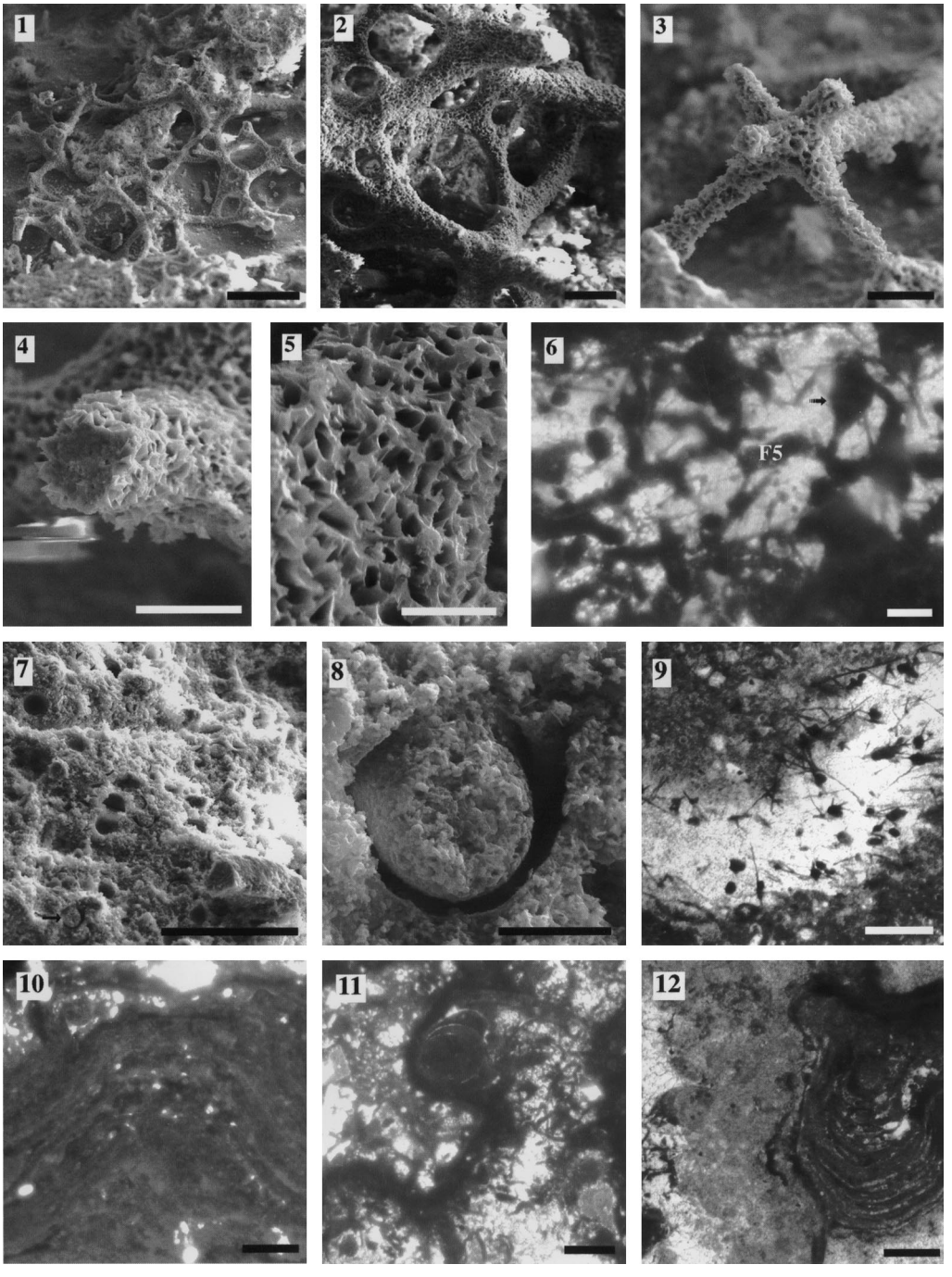
1
2
3
4
5
6
F5
7
8
9
10
11
12

The iron (hydr)oxides that are now hematite and goethite (as indicated from XRD analyses from the cortices of oncoids) preserved these biosedimentary structures, which are usually not preserved. Primary hematitization is also a possibility (Eren and Kadir, 1999). Early calcite cementation later filled the voids.

As in our previous studies in the European Paleozoic series, the general environment of oncoid growth is deep, well below the photic zone. This contrasts with other interpretations that suggest shallow to very shallow deposition for Mesozoic ferruginous oncoids. For Rioult et al. (1991) the environment at Sainte-Honorine-des-Pertes is subtidal to supratidal and the ferruginous oncoids are controlled by biological processes in the photic zone and by tidal currents on shoal bottoms. Gatrall et al. (1972) conclude in a similar manner for the limonitic concretions from the Jurassic of southern England. However, Palmer and Wilson (1990) suggest that the microorganisms involved in these English oncoids were non-photosynthetic. We suggest that the French oncoids developed during sea-level rises and that these grains were reworked by grazing organisms or eventually by episodic storm events. However, the ferruginous ooid grainstones (bed (b)) reflect higher-energy conditions and were probably formed in shallow environments in a distant shelf. They were reworked from this place, deposited deeper near the storm wave base and mixed with the former ferruginous oncoids.

4.2. Microfossils

Filamentous microfossils of types 1–4 resemble present-day filamentous bacteria. However, no conclusion can be drawn about their taxonomic position because morphology alone is not sufficient to identify bacterial taxa. Filamentous bacteria are frequently observed in modern iron deposits, both in fresh- and sea-water environments (Ghiorse, 1984; Juniper and Tebo, 1995; Gillan and De Ridder, 1997; Tazaki, 1998). These modern filamentous microbes, which form iron encrusted mats and biofilms, are identified as Beggiatoales e.g. *Thiothrix* and *Beggiatoa*, sheathed bacteria like *Sphaerotilus* and *Leptothrix*, and Cytophagaceae like *Flexibacter* and *Cytophaga*.

Because of their large diameter and their branching nature, filaments of type 5 are probably filamentous fungi. Another argument in favor of fungi is the presence of associated stalked bodies; they resemble zoosporangia and oogonia of some Oomycota (the spheroidal inclusions would be spores or eggs). Alternatively, stalked bodies could be sessile protozoans, like Suctoria. Filamentous fungi with branching mycelium occur in most waters (Rheinheimer, 1980). Some fungi are even known to precipitate iron in marine sediments and desert rock varnishes (Dahanayake and Krumbein, 1986).

Morphology alone is not sufficient to identify spheroidal bodies. However, the close association of these bodies with filaments of type 2 resemble Chytridiomycota. These microbes are filamentous fungi that form spheroidal sporangia of comparable size. Chytridiomycota are widely distributed in the marine environment (Rheinheimer, 1980).

The microfossils described grew in biofilms but were also endolithic. Both biofilm and endolithic microbes were incrusted with iron minerals. Shell-boring iron-encrusted bacterial filaments are known in present-day bivalves, for example in the oyster *Placuna placenta* (Raghukumar et al., 1989). Although the filamentous microbes associated with ferruginous oncoids and crusts cannot be identified taxonomically, their presence (and abundance) must be taken into account to explain the genesis of these sedimentary structures. Microbes are generally

Plate 7. Figures 1–9 from sample Shp6, similar to the one illustrated on Plate 1, 2. 1–4. Type 5 filaments. Acid-leached sections, SEM. ULB, Préat shp6(sem) (figure 1), Préat shp53(sem) (figure 2), Préat shp9(sem) (figure 3), Préat shp7(sem) (figure 4). Scale bars 500 μm (figure 1), 100 μm (figures 2–3), 50 μm (figure 4). 5. Surface of type 5 filaments. Acid-leached section, SEM. ULB, Préat shp8(sem), scale bar 10 μm. 6. Endolithic (?) type 5 filaments (F5). Arrow shows a stalked body. Polished section. ULB, photograph Préat 44/11, scale bar 100 μm. 7, 8. Spheroidal bodies (arrow in figure 7). Acid-leached sections, SEM. ULB, Préat shp15(sem) (figure 7) and Préat shp17(sem) (figure 8). Scale bars 100 μm (figure 7) and 10 μm (figure 8). 9. Endolithic (?) spheroidal bodies associated with type 2 filaments. Polished section. ULB, photograph Préat 45/34, scale bar 120 μm. 10–12. Microstromatolites. Polished sections. ULB, photograph Préat 44/21 Sample Shp7 (figure 10), photograph Préat 45/8 Sample Shp7 (figure 11), photograph Préat 45/25 Sample Shp7 (figure 12). See also Plate 1, 3 and Plate 5, 1–3. Scale bars 150 μm (figure 10), 140 μm (figure 11), 150 μm (figure 12).

abundant at solid/liquid interfaces where they form microbial communities called biofilms (Cooksey and Wigglesworth-Cooksey, 1995). As a consequence, at the time of deposition oncoid nuclei were probably covered with various microbes, some being shell-borers. The waters were deep, calm and dysaerobic and many interfaces were present. Microorganisms grew at these interfaces, consuming the remaining oxygen and producing various reduced catabolites. In such conditions, the stability of the soluble reduced state of iron (Fe^{2+}) was higher. Iron could thus serve as an electron donor in metabolism for iron-oxidizing bacteria that lived in biofilms. Iron-oxidizing bacteria are always abundant at such interfaces in modern environments where iron deposits are formed (Ehrlich, 1990).

However, biological iron-oxidation is not the only process that can lead to microbial iron deposition. For example, iron ions (Fe^{2+} and Fe^{3+}) may also be complexed by microbial exopolymeric substances (EPS); such complexation may be followed by nucleation of various iron minerals according to the redox conditions. Another possibility is microbial degradation of organic iron complexes (Gillan et al., 2000). Although the exact mechanism of iron deposition is not known, we show in the present work that iron minerals are closely associated with various filamentous microbes in the oncoid cortices, as well as in ferruginous crusts. Many shell fragments are also colonized by endolithic microbes. These observations suggest that microbes played an important role in the genesis of these sedimentary structures. Many filamentous bacteria are present at the surface of Modern ferromanganese nodules (Burnett and Nealson, 1981, 1983). The culture of iron precipitating bacteria from these nodules suggests that microorganisms play a direct role in their formation (Ghiorse and Hirsch, 1982). Ferromanganese nodules could thus correspond to modern analogs of the oncoids described in this work. Interestingly, ferromanganese nodules also form principally in deep, aphotic marine waters characterized by very slow sedimentation rates (Von Stackelberg, 1987).

5. Conclusions

The Oolite ferrugineuse de Bayeux is a marine ramp succession. The sequence is condensed, and is entirely deep as there is no evidence of shallow-water or subaerial exposure. The same conclusion applies to the ferruginous coated grains as they contain planktonic foraminifers. It is apparent that microbial activity played a significant role in the origin of various structures and coated grains in the Middle Jurassic sediments of Normandy. The described microbes grew in biofilms, but are also endolithic in various bioclasts, cavities and sedimentary figures. Both biofilm and endolithic microbes are incrusted with ferric iron minerals suggesting that they provide the iron of the coated grains. The main conclusions are that: (1) regardless of geological age (Paleozoic, Mesozoic or Recent) and geographical location, iron-rich structures (oncoids, hardgrounds, microstromatolites, etc) are associated with microbes, and (2) the paleoenvironment always features gradients of oxygen and Fe^{2+} along various sediment-water interfaces. These interfaces are either large as in the deep part of the marine realm (outer ramps or hemipelagic shelfs), or limited and local as, for example, in the burrows of the shallow subtidal and intertidal zones (see MF2, this study or the Recent *Echinocardium cordatum* and *Montacuta ferruginosa* burrows (Temara et al., 1993; Gillan and De Ridder, 1997)). The fossilized iron-encrusted bacteria and fungi are therefore possible indicators of anoxic to dysaerobic conditions in various paleo(micro)environments, where iron (and manganese) would occur in its soluble reduced state (Fe^{2+}). When dissolved oxygen increases, ferric (hydr)oxides are precipitated 'actively' or more passively on available nucleation sites such as those of bacteria and fungi. The red color of many stratified and unstratified carbonate bodies is probably linked to ancient microbial activity, and thus indicates a dysaerobic paleo(micro)environment.

Acknowledgements

Grateful acknowledgement is expressed to Prof. Alain Bernard (Université Libre de Bruxelles) for SEM and XRD analyses, and to the reviewers Dr N. James and R. Burkhalter. The investigations were supported by the Fonds National de la Recherche Scientifique (Project FRFC n°2-4515-99).

References

Boulvain, F., 1989. Origine microbienne du pigment ferrugineux des monticules micritiques du Frasnien de l'Ardenne. Ann. Soc. Géol. Belgique 112/1, 79–85.

Boulvain, F., (1993). Sédimentologie et diagenèse des monticules micritiques "F2j" du Frasnien de l'Ardenne. Prof. Paper, Serv. géol. Belgique, 2 fasc., 260, Bruxelles.

Bourque, P.A., Boulvain, F., 1993. A model for the origin and petrogenesis of the red *Stromatactis* limestone of Paleozoic carbonate mounds. J. Sediment. Petrol. 163/4, 574–588.

Bromley, R., 1990. Trace Fossils. Biology and Taphonomy, Unwin Hyman, London (280pp.).

Burkhalter, R.M., 1995. Ooidal ironstone and ferruginous microbialites: origin and relation to sequence stratigraphy (Aalenian and Bajocian, Swiss Jura mountains). Sedimentology 42, 57–74.

Burnett, B.R., Nealson, K.H., 1981. Organic films and microorganisms associated with manganese nodules. Deep-Sea Res. 28, 637–645.

Burnett, B.R., Nealson, K.H., 1983. Energy dispersive X-ray analysis of the surface of a deep-sea ferromanganese nodule. Mar. Geol. 53, 313–329.

Chafetz, H.S., Akdim, B., Julia, R., Reid, A., 1998. Mn- and Fe-rich black travertine shrubs: bacterially (and nanobacterially) induced precipitates. J. Sediment. Res. 68/3, 404–412.

Cooksey, K.E., Wigglesworth-Cooksey, B., 1995. Adhesion of bacteria and diatoms to surfaces in the sea: review. Aquat. Microbiol. Ecol. 9, 87–96.

Dahanayake, K., Krumbein, W.E., 1986. Microbial structures in oolitic iron formations. Min. Deposita 21, 85–94.

Dangeard, L., 1930. Récif et galet d'algues dans l'Oolithe ferrugineuse de Normandie. C. R. Acad. Sci. Paris 190, 66–68.

Ehrlich, H.L., 1990. Geomicrobiology of iron. In: Ehrlich, H.L. (Ed.). Geomicrobiology, 2nd ed. Marcel Dekker, New York, pp. 283–346.

Eren, M., Kadir, S., 1999. Colour origin of upper Cretaceous pelagic red sediments within the Eastern Pontides, northeast Turkey. Geol. Rundschau 88, 593–595.

Fernandez Lopez, S., 1991. Taphonomic concepts for a theoretical biochronology. Rev. Espan. Paleontol. 6, 37–49.

Fortin, D., Ferris, F.G., Beveridge, T.J., 1997. Surface-mediated mineral development by bacteria. In Banfield J.F., Nealson K.H. (Eds.), Geomicrobiology: interactions between microbes and minerals, Review in Mineralogy, 35, pp. 171–178.

Fürsich, F., 1971. Hartgründe und Kondensation im Dogger von Calvados. N. Jb. Geol. Paläont. Abh. 138/3, 313–342.

Fürsich, F., 1998. Environmental distribution of trace fossils in the Jurassic of Kachchh (Western India). Facies 39, 46–53.

Gatrall, M., Jenkyns, H.C., Parsons, C.F., 1972. Limonitic concretions from the European Jurassic, with particular reference to the 'Snuff-Boxes' of southern England. Sedimentology 18, 79–103.

Gauthier, H., Rioult, M., Trévian, M., 1995. Enregistrement biostratigraphique exceptionnel dans "l'Oolithe ferrugineuse de Bayeux" au Sud de Caen (Normandie, France): complément au stratotype du Bajocien. C.R. Acad. Sci. Paris 321 (II a), 317–323.

Ghiorse, W.C., 1984. Biology of iron- and manganese-depositing bacteria. Ann. Rev. Microbiol. 38, 515–550.

Ghiorse, W.C., Hirsch, P., 1982. Isolation and properties of ferromanganese-depositing budding bacteria from Baltic Sea ferromanganese concretions. Appl. Environ. Microbiol. 43, 1464–1472.

Gillan, D.C., De Ridder, C., 1995. The microbial community associated with *Montacuta ferruginosa*, a commensal bivalve of the echinoid *Echinocardium cordatum*. In: Emson, R.H., Smith, A.B., Campbell, A.C. (Eds.), Echinoderm Research, Balkema, Rotterdam, pp. 71–76.

Gillan, D.C., De Ridder, C., 1997. Morphology of a ferric iron-encrusted biofilm forming on the shell of a burrowing bivalve (Mollusca). Aquat. Microbiol. Ecol. 12, 1–10.

Gillan, D.C., Warnau, M., De Vrind-de Jong, E.W., Boulvain, F., Préat, A., De Ridder, C., 2000. Iron oxidation and deposition in the biofilm covering *Montacuta ferruginosa* (Mollusca, Bivalvia). Geomicrobiol. J. 17/2, 141–150.

Juniper, S.K., Tebo, B.M., 1995. Microbe-metal interactions and mineral deposition at hydrothermal vents. In: Karl, D.M. (Ed.). The Microbiology of Deep-Sea Hydrothermal Vents, CRC Press, USA, pp. 219–253.

Kimberley, M.M., 1978. Paleoenvironmental classification of iron formations. Econ. Geol. 73, 215–229.

Konhauser, K.O., 1998. Diversity of bacterial iron mineralization. Earth Sci. Rev. 43, 91–121.

Lockair, R.E., Savrda, C.E., 1998. Ichnofossil tiering analysis of a rhythmically bedded chalk-marl sequence in the Upper Cretaceous of Alabama. Lethaia (Oslo), 311–322.

Mamet, B., Boulvain, F., 1988. Remplissages bactériens de cavités biohermales frasniennes. Bull. Soc. Belge Géol. 97/1, 63–76.

Mamet, B., Boulvain, F., 1991. Constructions hématitiques des Griottes carbonifères (Asturies, Espagne). Bull. Soc. Belge Géol. 99/2, 229–239.

Mamet, B., Perret, C., 1995. Bioconstructions hématitiques de Griottes dévoniennes (Pyrénées centrales). Géobios 28/6, 655–661.

Mamet, B., Préat, A., De Ridder, C., 1997. Bacterial Origin of the Red Pigmentation in the Devonian Slivenec Limestone, Czech Republic. Facies 36, 173–188.

Nealson, K.H., 1983. The microbial iron cycle. In: Krumbein, W.E. (Ed.). Microbial Geochemistry, Blackwell Scientific Publications, Oxford, pp. 159–190.

d'Orbigny, A., 1849–1852. Cours élémentaire de Paléoécologie et de Géologie Stratigraphique. Masson, vol. 2, 846pp.

Palmer, T.J., Wilson, M., 1990. Growth of ferruginous oncoliths in the Bajocian (Middle Jurassic) of Europe. Terra Nova 2, 142–147.

Pavia, G., 1994. Taphonomic remarks on d'Orbigny's type Bajocian (Bayeux, west France). Miscellanea del Servizi geologico Nazionale 5, 93–111.

Préat, A., Mamet, B., Devleeschouwer, X., 1998. Sédimentologie du stratotype de la limite Frasnien-Famennien (Coumiac, Montagne Noire, France). Bull. Soc. Géol. France 169/3, 331–342.

Préat, A., Mamet, B., Bernard, A., Gillan, D.C., 1999a. Rôle des organismes microbiens et des constructions hématitiques dans la

formation des matrices rougeâtres de différentes séries paléozoïques d'Europe: l'exemple du Dévonien de la Montagne Noire. Rev. Micropal. 42/2, 161–182.

Préat, A., Mamet, B., Bernard, A., Gillan, D.C., 1999b. Bacterial mediation, red matrices diagenesis, Devonian, Montagne Noire (southern France). Geol. Sediment. 126/1-4, 223–243.

Raghukumar, C., Rao, V.P.C., Iyer, S.D., 1989. Precipitation of iron in windowpane oyster shells by marine shell-boring cyanobacteria. Geomicrobiol. J. 7, 235–244.

Rheinheimer, G. (Ed.), 1980. Aquatic Microbiology, Wiley, New York, 235pp.

Rioult, M., 1964. Le stratotype du Bajocien. Coll. Jurassique, Luxembourg 1962. Publ. Inst. Grand Ducal Luxembourg. Sci. Nat. Phys. Math., 239–258.

Rioult, M., Dugué, O., Jan du Chêne, R., Ponsot, C., Fily, G., Moron, J.M., Vail, P.R., 1991. Outcrop sequence stratigraphy of the Anglo-Paris Basin, Middle to Upper Jurassic (Normandy, Maine, Dorset). Bull. Centres Rech. Explor.-Prod. Elf Aquitaine 15/1, 101–194.

Tazaki, K. 1998. A new world in the science of biomineralization. Environmental biomineralization in microbial mats, in Japan. Tazaki K. (Ed.), The Science Reports of Kanazawa University, Japan, XLII, no 1, 2.

Temara, A., De Ridder, C., Kuenen, J.G., Robertson, L.A., 1993. Sulfide-oxidizing bacteria in the burrowing echinoid *Echinocardium cordatum* (Echinodermata). Mar. Biol. 115, 179–185.

Von Stackelberg, U., 1987. In: Teleki, P.G., Dobson, M.R., Moore, J.R., Von Stackelberg, U. (Eds.). Growth History and Variability of Manganese Nodules of the equatorial North Pacific, Marine Minerals, Advance in Research and Resource Assesment, 194. NATO ASI Series, Ser. C, pp. 198–204.

Young, T.P., 1989. Phanerozoic ironstones: an introduction and review. In: Young, T.P., Taylor, W.E.G. (Eds.). Phanerozoic Ironstones, vol. 46. Spec. Publ. Geol. Soc. London, London, pp. 9–25.